

Subset Simulation and its Application to Seismic Risk Based on Dynamic Analysis

S. K. Au¹ and J. L. Beck²

Abstract: A method is presented for efficiently computing small failure probabilities encountered in seismic risk problems involving dynamic analysis. It is based on a procedure recently developed by the writers called Subset Simulation in which the central idea is that a small failure probability can be expressed as a product of larger conditional failure probabilities, thereby turning the problem of simulating a rare failure event into several problems that involve the conditional simulation of more frequent events. Markov chain Monte Carlo simulation is used to efficiently generate the conditional samples, which is otherwise a nontrivial task. The original version of Subset Simulation is improved by allowing greater flexibility for incorporating prior information about the reliability problem so as to increase the efficiency of the method. The method is an effective simulation procedure for seismic performance assessment of structures in the context of modern performance-based design. This application is illustrated by considering the failure of linear and nonlinear hysteretic structures subjected to uncertain earthquake ground motions. Failure analysis is also carried out using the Markov chain samples generated during Subset Simulation to yield information about the probable scenarios that may occur when the structure fails.

DOI: 10.1061/(ASCE)0733-9399(2003)129:8(901)

CE Database subject headings: Markov chains; Reliability; Simulation; Algorithms; Seismic effects; Dynamic analysis.

Introduction

In modern performance-based engineering design, the proper assessment of the performance of structures constitutes an important component (SEAOC 1995, 2000; Cornell 1996; Wen 2000). This includes realistic modeling of material constitutive behavior, structural components, loading conditions, mechanism of deterioration, and so on, that are anticipated during the working life of a structure. Due to incomplete information, uncertainty always exist in the loading conditions as well as the structural behavior. A probabilistic approach allows scientific and engineering predictions to be made with different degrees of confidence reflecting the incomplete information available. Application of probability concepts to structural safety was initiated in the mid 1940s, due to the work of Freudenthal and his coworkers (Freudenthal 1947; Freudenthal 1956; Freudenthal et al. 1966).

Structural reliability is concerned with the probability that a structure will not reach some specified failure state in some uncertain environment. This problem can be posed mathematically as follows. Let $\theta \in R^n$ be a parameter vector containing all the uncertain quantities of interest; in general, they will relate to the structural behavior and the loading conditions. Let $q: R^n \rightarrow [0, \infty)$ be a prescribed probability density function (PDF) quantifying the

relative plausibility of values that the set of uncertain parameters $\theta = [\theta_1, \dots, \theta_n]$ may assume (Cox 1961). Without loss of generality, it is assumed that these parameters are, or can be transformed to be, independent, i.e., $q(\theta) = \prod_{j=1}^n q_j(\theta_j)$, where $q_j: R^1 \rightarrow [0, \infty)$ is the one-dimensional PDF for each θ_j . The failure probability can be formulated in a generic form as

$$P(F) = \int I_F(\theta) q(\theta) d\theta \quad (1)$$

where $F \subset R^n =$ failure region; and $I_F: R^n \rightarrow \{0, 1\} =$ indicator function: $I_F(\theta) = 1$ if $\theta \in F$ and $I_F(\theta) = 0$ otherwise. In Eq. (1), and throughout the paper, $P(F)$ denotes the probability that $\theta \in F$ where the probability distribution of θ is $q(\theta)$. Much attention has been given to the evaluation of the failure probability in the past few decades (e.g., Schuëller and Stix 1987; Engelund and Rackwitz 1993; Schuëller et al. 1993), which constitutes the domain of reliability methods.

Monte Carlo simulation methods (Hammersley and Handscorn 1964; Rubinstein 1981; Fishman 1996) offer a simple and robust means for estimating the failure probability for a specified structure and loading conditions, regardless of the complexity of the problem. In this approach, the failure probability in Eq. (1) is viewed as an expectation of the indicator function $I_F(\theta)$ where θ is distributed as q . "Random realizations," or "samples," of the uncertain parameters in the problem are generated according to their PDF. The failure probability is then estimated by the sample average of $I_F(\theta)$ which is just the fraction of the number of samples that lead to failure. Checking whether the structure has failed for each sample usually requires a structural analysis. As is well known, standard Monte Carlo simulation (MCS) is not computationally efficient for estimating small failure probabilities, since the number of samples required to achieve a given accuracy is inversely proportional to the failure probability when it is small. Essentially, estimating small probabilities requires information from rare samples which lead to failure, and on average it requires many samples before one such failure sample occurs.

¹School of Civil and Environmental Engineering, Nanyang Technological Univ., Singapore 639798.

²Division of Engineering and Applied Science, California Institute of Technology, Pasadena, CA 91125 (corresponding author). E-mail: jimbeck@caltech.edu

Note. Associate Editor: George Deodatis. Discussion open until January 1, 2004. Separate discussions must be submitted for individual papers. To extend the closing date by one month, a written request must be filed with the ASCE Managing Editor. The manuscript for this paper was submitted for review and possible publication on January 7, 2002; approved on November 21, 2002. This paper is part of the *Journal of Engineering Mechanics*, Vol. 129, No. 8, August 1, 2003. ©ASCE, ISSN 0733-9399/2003/8-901-917/\$18.00.

In view of the rare-event aspect of the standard Monte Carlo method, the importance sampling method (Rubinstein 1981; Schuëller and Stix 1987) has been introduced, which basically chooses an importance sampling distribution to generate samples that lead to failure more frequently. The efficiency of the method relies on a proper choice of the importance sampling distribution, which inevitably requires some knowledge about failure. Importance sampling has been successfully applied to time-invariant or static reliability problems where the number of uncertain parameters in the problem is not too large (Schuëller and Stix 1987; Bucher 1988; Melchers 1989; Papadimitriou et al. 1997; Der Kiureghian and Dakessian 1998; Au et al. 1999; Au and Beck 1999). For time-dependent problems, which are often characterized by a large number of uncertain parameters with complexity arising from its dynamic nature, the application of importance sampling is much more difficult (Au and Beck 2002). By exploiting knowledge of the failure region, Au and Beck (2001b) have developed a very efficient importance sampling method for the first-excursion problem for linear dynamical systems under Gaussian stochastic excitation. However, efficient and robust simulation methods for solving general time-dependent reliability problems are still at their early exploration stage (Schuëller et al. 1993).

This study is based on a simulation-based reliability method, called *Subset Simulation*, that was developed recently to efficiently compute the small failure probabilities encountered in engineering reliability analysis of general dynamical systems (Au and Beck 2001a). The method presented in this paper is an improved version of Subset Simulation that utilizes the Metropolis-Hastings algorithm for generating conditional samples; it offers greater flexibility for incorporating prior information about the reliability problem into the simulation procedure in order to improve efficiency of the method. Subset Simulation is an effective simulation procedure for seismic performance assessment of structures. This application is illustrated by considering the first-excursion failure of linear and nonlinear hysteretic structures subjected to uncertain earthquake ground motions.

Basic Idea of Subset Simulation

Given a failure region F , let $F_1 \supset F_2 \supset \dots \supset F_m = F$ be a decreasing nested sequence of failure regions so that $F_k = \bigcap_{i=1}^k F_i$, $k = 1, \dots, m$. For example, if failure of a system is defined as the exceedance of an uncertain demand D over a given capacity C , that is, $F = \{\theta: D(\theta) > C(\theta)\}$, then an appropriate sequence of nested failure regions can simply be defined as $F_i = \{\theta: D(\theta) > C_i(\theta)\}$, where $C_1 < C_2 < \dots < C_m = C$. By definition of conditional probability, we have

$$\begin{aligned}
 P(F) &= P(F_m) = P(\bigcap_{i=1}^m F_i) = P(F_m | \bigcap_{i=1}^{m-1} F_i) P(\bigcap_{i=1}^{m-1} F_i) \\
 &= P(F_m | F_{m-1}) P(\bigcap_{i=1}^{m-1} F_i) = \dots = P(F_1) \prod_{i=1}^{m-1} P(F_{i+1} | F_i)
 \end{aligned} \tag{2}$$

Eq. (2) expresses the failure probability as a product of a sequence of conditional probabilities $\{P(F_{i+1} | F_i): i = 1, \dots, m-1\}$ and $P(F_1)$. The idea of Subset Simulation is to estimate the failure probability $P(F)$ by estimating these quantities.

Standard MCS can be used to estimate $P(F_1)$ and it is natural to compute the conditional failure probabilities in Eq. (2) based on a similar approach, which necessitates the simulation of

samples according to the conditional distribution of θ given that it lies in F_i , that is, $q(\theta | F_i) = q(\theta) I_{F_i}(\theta) / P(F_i)$. This is in general a highly nontrivial task. Nevertheless, it is found (Au and Beck 2001a) that Markov Chain Monte Carlo (MCMC) simulation provides a powerful method for simulating samples conditional on the failure region F_i ($i = 1, \dots, m-1$). A MCMC method based on the modified Metropolis algorithm was developed in previous work (Au and Beck 2001a). This paper presents a generalized MCMC scheme which is based on the Metropolis-Hastings algorithm. The generalization allows more information about the reliability problem to be incorporated into the simulation procedure so as to improve efficiency of the method.

Markov Chain Monte Carlo Simulation

Markov Chain Monte Carlo simulation is a class of powerful simulation techniques for generating samples according to any given probability distribution. It originates from the method developed by Metropolis and his coworkers for applications in statistical physics (Metropolis et al. 1953). A major generalization of the Metropolis method was due to Hastings for applications in Bayesian statistics (Hastings 1970). See Fishman (1996) for a comprehensive discussion of MCMC methods. Applications to reliability calculations and Bayesian system identification in civil engineering include Au and Beck (1999), Au and Beck (2001a) and Beck and Au (2002).

The significance of MCMC simulation to solving reliability problems is that it provides a versatile way for generating samples according to the conditional PDF $q(\theta | F)$, which has been the main challenge in a simulation-based reliability method. Successive samples are generated from a specially designed Markov chain. Assuming the algorithm is properly implemented so that the Markov chain is ergodic (Au and Beck 2001a), the distribution of the samples tends to the conditional PDF $q(\theta | F)$ as the length of the Markov chain increases. Specifically, let $\{\theta_1, \theta_2, \dots\}$ be the Markov chain samples, then θ_n is distributed as $q(\theta | F)$ as $n \rightarrow \infty$. If the initial sample θ_1 is distributed exactly as the conditional PDF $q(\theta | F)$, then so are the subsequent samples $\{\theta_2, \theta_3, \dots\}$ and the Markov chain is always in a stationary state; as shown later, this is the case for Subset Simulation. The Markov chain samples can be used for statistical averaging to yield estimates for the conditional expectation of quantities of interest.

The proposed MCMC scheme for generating samples with limiting stationary PDF equal to $q(\theta | F)$ is presented as follows. In applications, the parameters in the uncertain parameter vector θ naturally fall into groups, as will be seen later in the examples. Let $I = \{I_1, \dots, I_{n_G}\}$, where n_G is the number of groups, be the grouping (or partition) of the indices $\{1, \dots, n\}$ corresponding to the uncertain parameters $\{\theta_1, \dots, \theta_n\}$. Without loss of generality, we can assume that the indices are numbered so that their numerical order is not affected by grouping. For example, a valid grouping of $\{1, \dots, 6\}$ is $(\{1,2\}, \{3\}, \{4,5,6\})$, for which $I_1 = \{1,2\}$, $I_2 = \{3\}$, $I_3 = \{4,5,6\}$, and $n_G = 3$. Let $\theta^{(j)} \in \mathbb{R}^{n_j}$ be the set of the n_j parameters in the j th group ($j = 1, \dots, n_G$). The whole set of uncertain parameters θ consists of members from all the groups, that is, $\theta = [\theta^{(1)}, \dots, \theta^{(n_G)}] \in \mathbb{R}^n$. For each group j , let $q^{(j)}(\theta^{(j)}) = \prod_{r \in I_j} q_r(\theta_r)$ be the PDF for the j th group. The final ingredient is a "proposal PDF" $p_j^*(\xi^{(j)} | \theta^{(j)}): \mathbb{R}^{n_j} \times \mathbb{R}^{n_j} \rightarrow [0, \infty)$ which is chosen for each group to generate a random "precandidate component" $\xi^{(j)} \in \mathbb{R}^{n_j}$ based on the current sample component $\theta^{(j)} \in \mathbb{R}^{n_j}$ (see later for the choice of proposal PDF). To generate the

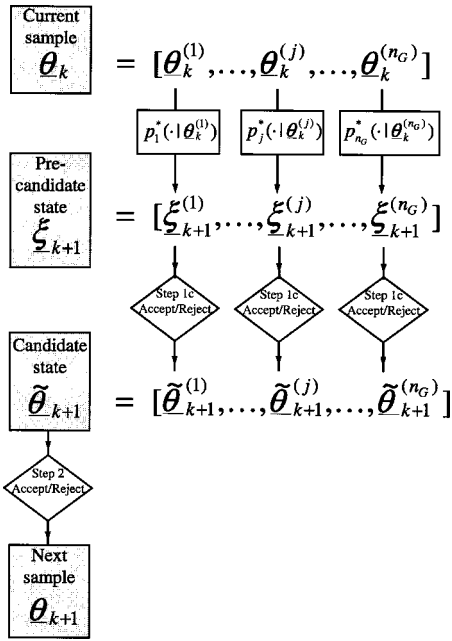


Fig. 1. Illustration of modified Metropolis-Hastings algorithm

next Markov chain sample $\underline{\theta}_{k+1} = [\underline{\theta}_{k+1}^{(1)}, \dots, \underline{\theta}_{k+1}^{(n_G)}]$ from the current sample $\underline{\theta}_k = [\underline{\theta}_k^{(1)}, \dots, \underline{\theta}_k^{(n_G)}]$, the following algorithm is applied:

Modified Metropolis-Hastings Algorithm

1. Generate a candidate state $\tilde{\theta}_{k+1} = [\tilde{\theta}_{k+1}^{(1)}, \dots, \tilde{\theta}_{k+1}^{(n_G)}]$:
For each group $j = 1, \dots, n_G$,
 - Generate a precandidate component $\xi_{k+1}^{(j)}$ from $p_j^*(\cdot | \underline{\theta}_k^{(j)})$
 - Compute the acceptance ratio:

$$r_{k+1}^{(j)} = \frac{q^{(j)}(\xi_{k+1}^{(j)}) p_j^*(\underline{\theta}_k^{(j)} | \xi_{k+1}^{(j)})}{q^{(j)}(\underline{\theta}_k^{(j)}) p_j^*(\xi_{k+1}^{(j)} | \underline{\theta}_k^{(j)})} \quad (3)$$

- Set $\tilde{\theta}_{k+1}^{(j)}$, the j th component of $\tilde{\theta}_{k+1}$, according to

$$\tilde{\theta}_{k+1}^{(j)} = \begin{cases} \xi_{k+1}^{(j)} & \text{with probability } \min(1, r_{k+1}^{(j)}) \\ \underline{\theta}_k^{(j)} & \text{with probability } 1 - \min(1, r_{k+1}^{(j)}) \end{cases} \quad (4)$$

2. Accept/reject candidate state $\tilde{\theta}_{k+1}$:

If $\tilde{\theta}_{k+1} = \underline{\theta}_k$ (i.e., no precandidate components were accepted), set $\underline{\theta}_{k+1} = \underline{\theta}_k$. Otherwise, check the location of $\tilde{\theta}_{k+1}$ by performing a structural analysis. If $\tilde{\theta}_{k+1} \in F$, accept it as the next state, i.e., set $\underline{\theta}_{k+1} = \tilde{\theta}_{k+1}$; otherwise, reject it and take the current state as the next one, i.e., set $\underline{\theta}_{k+1} = \underline{\theta}_k$.

Fig. 1 gives a schematic illustration of the algorithm.

It should be noted that when every uncertain parameter is grouped individually (i.e., there are as many groups as the number of uncertain parameters) and the proposal PDFs are all symmetric [i.e., $p_j^*(\xi_j; \theta_j) = p_j^*(\theta_j; \xi_j)$ for all $j = 1, \dots, n$], then the current algorithm reduces to the modified Metropolis algorithm presented in previous work (Au and Beck 2001a).

Proof of Stationary Distribution

Since the same rule is used to generate the next sample from the current one regardless of the Markov step k , the transition probability $p(\underline{\theta}_{k+1} | \underline{\theta}_k)$ of the Markov chain is stationary, that is, in-

dependent of k . We next show that if $\underline{\theta}_k$ is distributed as the target PDF $q(\underline{\theta} | F)$, then so is $\underline{\theta}_{k+1}$, and hence $q(\underline{\theta} | F)$ is a stationary distribution of the Markov chain.

As all the Markov chain samples lie in F as enforced by Step 2, it suffices to consider the transition between the states in F , which is governed by Step 1. According to Step 1, the transition of the individual groups are independent, so the transition PDF of the Markov chain between any two states in F can be expressed as a product of the group transition PDFs

$$p(\underline{\theta}_{k+1} | \underline{\theta}_k) = \prod_{j=1}^{n_G} p_j(\underline{\theta}_{k+1}^{(j)} | \underline{\theta}_k^{(j)}) \quad (5)$$

where p_j = transition PDF for the j th component $\underline{\theta}_k^{(j)}$ of $\underline{\theta}_k$. First, consider the transition between distinct states for the j th group, i.e., $\underline{\theta}_k^{(j)} \neq \underline{\theta}_{k+1}^{(j)}$, then

$$p_j(\underline{\theta}_{k+1}^{(j)} | \underline{\theta}_k^{(j)}) = p_j^*(\underline{\theta}_{k+1}^{(j)} | \underline{\theta}_k^{(j)}) \min\{1, r_{k+1}^{(j)}\} \quad (6)$$

Substituting Eq. (3) into Eq. (6), and using the identity $\min\{1, a/b\} b = \min\{1, b/a\} a$ for any positive numbers a and b , it is straightforward to show that p_j satisfies the following “reversibility condition” with respect to $q^{(j)}$:

$$p_j(\underline{\theta}_{k+1}^{(j)} | \underline{\theta}_k^{(j)}) q^{(j)}(\underline{\theta}_k^{(j)}) = p_j(\underline{\theta}_k^{(j)} | \underline{\theta}_{k+1}^{(j)}) q^{(j)}(\underline{\theta}_{k+1}^{(j)}) \quad (7)$$

Next, note that the equality in Eq. (7) is trivial when $\underline{\theta}_{k+1}^{(j)} = \underline{\theta}_k^{(j)}$. Thus, Eq. (7) holds in general, for each group $j = 1, \dots, n_G$. Combining Eqs. (5) and (7), and the fact that all states lie in F , the transition PDF for the whole state $\underline{\theta}_k$ also satisfies the following reversibility condition with respect to $q(\cdot | F)$:

$$p(\underline{\theta}_{k+1} | \underline{\theta}_k) q(\underline{\theta}_k | F) = p(\underline{\theta}_k | \underline{\theta}_{k+1}) q(\underline{\theta}_{k+1} | F) \quad (8)$$

Thus, if the current sample $\underline{\theta}_k$ is distributed as $q(\cdot | F)$, then

$$\begin{aligned} p(\underline{\theta}_{k+1}) &= \int p(\underline{\theta}_{k+1} | \underline{\theta}_k) q(\underline{\theta}_k | F) d\underline{\theta}_k \\ &= \int p(\underline{\theta}_k | \underline{\theta}_{k+1}) q(\underline{\theta}_{k+1} | F) d\underline{\theta}_k \text{ by Eq. (8)} \\ &= q(\underline{\theta}_{k+1} | F) \int p(\underline{\theta}_k | \underline{\theta}_{k+1}) d\underline{\theta}_k = q(\underline{\theta}_{k+1} | F) \end{aligned} \quad (9)$$

since $\int p(\underline{\theta}_k | \underline{\theta}_{k+1}) d\underline{\theta}_k = 1$. This shows that the next Markov chain sample $\underline{\theta}_{k+1}$ will also be distributed as $q(\cdot | F)$, and so the latter is indeed a stationary distribution for the generated Markov chain, regardless of the choice of the proposal PDF p_j^* for each group in the proposed MCMC algorithm.

Subset Simulation Procedure

Utilizing the modified Metropolis-Hastings method developed in the last section, Subset Simulation proceeds as follows. First, we simulate N samples $\{\theta_1, \dots, \theta_N\}$ by standard MCS to compute an estimate \tilde{P}_1 for $P(F_1)$ by

$$P(F_1) \approx \tilde{P}_1 = \frac{1}{N} \sum_{k=1}^N \mathbb{I}_{F_1}(\theta_k) \quad (10)$$

where $\{\theta_k : k = 1, \dots, N\}$ are independent and identically distributed (i.i.d.) samples simulated according to the parameter PDF q . From these MCS samples, we can readily obtain some samples distributed as $q(\cdot | F_1)$, simply as those that lie in F_1 . Starting from each of these samples, we can simulate Markov chain

samples using the modified Metropolis-Hastings method. As shown in the previous section, these samples will also be distributed as $q(\cdot|F_1)$ because the Markov chain is in a stationary state. They can be used to estimate $P(F_2|F_1)$ using an estimator \tilde{P}_2 similar to Eq. (10). Observe that the Markov chain samples, which lie in F_2 are distributed as $q(\cdot|F_2)$ and thus they provide “seeds” for simulating more samples according to $q(\cdot|F_2)$ to estimate $P(F_3|F_2)$. Repeating this process, we can compute the conditional probabilities of the higher-conditional levels until the failure region of interest $F (=F_m)$ has been reached. At the i th conditional level, $1 \leq i \leq m-1$, let $\{\theta_{i,k}: k=1, \dots, N\}$ be the Markov chain samples with distribution $q(\cdot|F_i)$, possibly coming from different chains generated by different “seeds.” Then

$$P(F_{i+1}|F_i) \approx \tilde{P}_{i+1} = \frac{1}{N} \sum_{k=1}^N \mathbb{I}_{F_{i+1}}(\theta_{i,k}) \quad (11)$$

Finally, combining Eqs. (2), (10), and (11), the failure probability estimator is

$$\tilde{P}_F = \prod_{i=1}^m \tilde{P}_i \quad (12)$$

Notice that the total number of samples generated is $N_T = mN$ where m is the number of levels and N is the number of samples generated for each level.

Statistical Properties of Estimators

In this section, we present results on the statistical properties of the estimators \tilde{P}_i ($i=1, \dots, m$) and \tilde{P}_F . The detailed derivation of these results can be found in Au and Beck (2001a) or Au (2001).

Monte Carlo Simulation Estimator \tilde{P}_1

As is well-known, the MCS estimator \tilde{P}_1 in (10) computed using the i.i.d. samples $\{\theta_1, \dots, \theta_N\}$ is unbiased. The coefficient of variation (c.o.v.) of \tilde{P}_1 , δ_1 , defined as the ratio of the standard deviation to the mean of \tilde{P}_1 , is given by

$$\delta_1 = \sqrt{\frac{1 - P(F_1)}{P(F_1)N}} \quad (13)$$

Conditional Probability Estimator \tilde{P}_i ($2 \leq i \leq m$)

Since the Markov chains generated at each conditional level are started with samples distributed as the corresponding target conditional PDF, the Markov chain samples used for computing the conditional probability estimators based on Eq. (11) are all identically distributed as the target conditional PDF. It follows that the conditional probability estimators \tilde{P}_i ($2 \leq i \leq m$) are unbiased. The c.o.v. of \tilde{P}_i , denoted by δ_i , is given by

$$\delta_i = \sqrt{\frac{1 - P(F_i|F_{i-1})}{P(F_i|F_{i-1})N}} (1 + \gamma_i) \quad (14)$$

where

$$\gamma_i = 2 \sum_{k=1}^{N/N_c - 1} \left(1 - \frac{kN_c}{N}\right) \rho_i(k) \quad (15)$$

is a correlation factor. It has been assumed that at each simulation level, there are N_c Markov chains developed, each having N/N_c

samples so that the total number of samples generated at each simulation level is $N_c \times N/N_c = N$ (the question of how to maintain a fixed number of chains N_c will be discussed later). In Eq. (15),

$$\rho_i(k) = R_i(k)/R_i(0) \quad (16)$$

is the correlation coefficient at lag k of the stationary sequence $\{I_{F_i}(\theta_{i-1,j,k}): k=1, \dots, N/N_c\}$, where $\theta_{i-1,j,k}$ denotes the k th sample along the j th chain (started from the j th seed) at the $(i-1)$ -th simulation level

$$\begin{aligned} R_i(k) &= \mathbb{E}[I_{F_i}(\theta_{i-1,j,1}) - P(F_i|F_{i-1})][I_{F_i}(\theta_{i-1,j,1+k}) \\ &\quad - P(F_i|F_{i-1})] \\ &= \mathbb{E}[I_{F_i}(\theta_{i-1,j,1})I_{F_i}(\theta_{i-1,j,1+k})] - P(F_i|F_{i-1})^2 \end{aligned} \quad (17)$$

is the covariance between $I_{F_i}(\theta_{i-1,j,1})$ and $I_{F_i}(\theta_{i-1,j,1+k})$, for any $l=1, \dots, N/N_c$, and it is independent of l due to stationarity. It is also independent of the chain index j since all chains are probabilistically equivalent.

The covariance sequence $\{R_i(k): k=1, \dots, N/N_c-1\}$ can be estimated using the Markov chain samples $\{\theta_{i-1,j,k}: j=1, \dots, N_c; k=1, \dots, N/N_c\}$ at the $(i-1)$ -th conditional level by

$$\begin{aligned} R_i(k) &\approx \tilde{R}(k) \\ &= \left(\frac{1}{N - kN_c} \sum_{j=1}^{N_c} \sum_{l=1}^{N/N_c - k} I_{F_i}(\theta_{i-1,j,l}) I_{F_i}(\theta_{i-1,j,l+k}) \right) - \tilde{P}_i^2 \end{aligned} \quad (18)$$

from which the correlation sequence $\{\rho_i(k): k=1, \dots, N/N_c-1\}$ and hence the correlation factor γ_i in Eq. (15) can also be estimated. Consequently, the c.o.v. δ_i for the conditional probability estimator \tilde{P}_i can be estimated by Eq. (14), where $P(F_i|F_{i-1})$ is approximated by \tilde{P}_i using Eq. (11).

Failure Probability Estimator \tilde{P}_F

Due to the correlation among the estimators $\{\tilde{P}_i: i=1, \dots, m\}$, \tilde{P}_F given by Eq. (12) is biased for every N . This correlation is due to the fact that the samples used for computing \tilde{P}_i which lie in F_i are used to start the Markov chains to compute \tilde{P}_{i+1} . It can be shown that the fractional bias of \tilde{P}_F is bounded by

$$\left| \mathbb{E} \left[\frac{\tilde{P}_F - P(F)}{P(F)} \right] \right| \leq \sum_{i>j} \delta_i \delta_j + o(1/N) = O(1/N) \quad (19)$$

which means that \tilde{P}_F is asymptotically unbiased and the bias is $O(1/N)$.

On the other hand, the c.o.v. δ of \tilde{P}_F may be bounded above by using

$$\delta^2 = \mathbb{E} \left[\frac{\tilde{P}_F - P(F)}{P(F)} \right]^2 \leq \sum_{i,j=1}^m \delta_i \delta_j + o(1/N) = O(1/N) \quad (20)$$

showing that \tilde{P}_F is a consistent estimator and its c.o.v. δ is $O(1/\sqrt{N})$. Note that the c.o.v. δ in Eq. (20) is defined through the expected deviation about the target failure probability $P(F)$ instead of $\mathbb{E}[\tilde{P}_F]$ so that the effects of bias are accounted for. The upper bound corresponds to the case when the conditional prob-

ability estimators $\{\bar{P}_i: i=2, \dots, m\}$ are fully correlated. The actual c.o.v. depends on the correlation between the \bar{P}_i s. If all the \bar{P}_i s were uncorrelated, then

$$\delta^2 = \sum_{i=1}^m \delta_i^2 \quad (21)$$

Although the \bar{P}_i s are generally correlated, simulations show that δ^2 may be well approximated by Eq. (21). This will be illustrated in the examples.

Implementation Issues

Choice of Intermediate Failure Regions

The choice of the intermediate failure regions $\{F_i: i=1, \dots, m-1\}$ plays a key role in the Subset Simulation procedure. Two issues are basic to their choice. The first is a parametrization of the target failure region F which allows the generation of intermediate failure regions by varying the value of the defined parameter. The second issue is the choice of the specific sequence of values of the defined parameter, which affects the values of the conditional probabilities $\{P(F_{i+1}|F_i): i=1, \dots, m-1\}$ and hence the efficiency of the Subset Simulation procedure.

Generic Representation of Failure Regions

Many failure regions encountered in engineering applications are a combination of the union and intersection of failure regions of components. In particular, consider a failure region F of the following form:

$$F = \bigcup_{j=1}^L \bigcap_{k=1}^{L_j} \{\theta: D_{jk}(\theta) > C_{jk}(\theta)\} \quad (22)$$

where $D_{jk}(\theta)$ and $C_{jk}(\theta)$ may be viewed as the demand and capacity variables of the (j, k) component of the system. The failure region F in Eq. (22) can be considered as the failure of a system with L subsystems connected in series, where the j th subsystem consists of L_j components connected in parallel.

In order to apply Subset Simulation, it is desirable to parameterize F with a single parameter so that the sequence of intermediate failure regions $\{F_i: i=1, \dots, m-1\}$ can be generated by varying the parameter. This can be accomplished as follows. For the failure region F in Eq. (22), define the ‘‘critical demand-to-capacity ratio’’ (CDCR) Y as

$$Y(\theta) = \max_{j=1, \dots, L} \min_{k=1, \dots, L_j} \frac{D_{jk}(\theta)}{C_{jk}(\theta)} \quad (23)$$

then it can be easily verified that

$$F = \{\theta: Y(\theta) > 1\} \quad (24)$$

and so the sequence of intermediate failure regions can be generated as

$$F_i = \{\theta: Y(\theta) > y_i\} \quad (25)$$

where $0 < y_1 < \dots < y_m = 1$ is a sequence of (normalized) intermediate threshold values. It is noted that although the intermediate failure regions are introduced purely for computational reasons in Subset Simulation, they may be viewed as corresponding to failure if the component capacities C_{jk} were all less by the same factor y_i than the specified values.

It is straightforward to generalize to failure regions consisting of multiple stacks of union and intersection. Essentially, Y is de-

finied using ‘‘max’’ and ‘‘min’’ in the same order corresponding to each occurrence of union (\cup) and intersection (\cap) in F , respectively.

Choice of Intermediate Threshold Levels

The choice of the sequence of intermediate threshold values $\{y_1, \dots, y_m\}$ appearing in the parameterization of intermediate failure regions affects the values of the conditional probabilities and hence the efficiency of the Subset Simulation procedure. If the sequence increases slowly, then the conditional probabilities will be large, and so their estimation requires less samples N . A slow sequence, however, requires more simulation levels m to reach the target failure region, increasing the total number of samples $N_T = mN$ in the whole procedure. Conversely, if the sequence increases too rapidly that the conditional failure events become rare, it will require more samples N to obtain an accurate estimate of the conditional failure probabilities in each simulation level, which again increases the total number of samples. It can thus be seen that the choice of the intermediate threshold values is a trade-off between the number of samples required in each simulation level and the number of simulation levels required to reach the target failure region.

One strategy for the choice of the intermediate threshold values is to choose the y_i a priori, but then it is difficult to control values of the conditional probabilities $P(F_i|F_{i-1})$. In this work, the y_i are chosen ‘‘adaptively’’ so that the estimated conditional probabilities are equal to a fixed value $p_0 \in (0, 1)$. This is accomplished by choosing the intermediate threshold level y_i ($i = 1, \dots, m-1$) as the $(1-p_0)N$ th largest value (i.e., an order statistic) among the CDCRs $\{Y(\theta_{i-1,k}): k=1, \dots, N\}$ where the $\theta_{i-1,k}$ are the Markov chain samples generated at the $(i-1)$ th conditional level for $i=2, \dots, m-1$, and the $\theta_{0,k}$ are the samples from the initial Monte Carlo simulation. This choice of the intermediate threshold levels implies that they are dependent on the conditional samples and will vary in different simulation runs. For a target probability level of 10^{-3} to 10^{-6} , choosing $p_0=0.1$ is found to yield good efficiency.

Using this adaptive choice of the proposal PDF, the Subset Simulation procedure is illustrated in Fig. 2 for simulation Level 0 (MCS) and Level 1 (MCMC).

Grouping of Uncertain Parameters and Choice of Proposal Probability Density Functions

The Subset Simulation method presented here differs from the previous version (Au and Beck 2001a) in that it allows grouping of uncertain parameters; the previous version corresponds to the special case where each uncertain parameter is in its own group.

The grouping of uncertain parameters and the choice of the group proposal PDFs affect the distribution and the acceptance rate of the candidate state. These in turn affect the correlation among the Markov chain samples [through the factor γ_i in Eq. (15)] and consequently the efficiency of the Subset Simulation procedure. They are the major channels through which prior knowledge about a particular problem can be used to improve the efficiency of the MCMC method.

Ideally, all uncertain parameters should be collected in one group and the proposal PDF should be chosen as the conditional PDF $q(\theta|F_i)$, in which case all states generated by the proposal PDF will be i.i.d. and accepted. Of course, this choice is not feasible, because an efficient algorithm for generating conditional samples is generally not available. The art of choosing the pro-

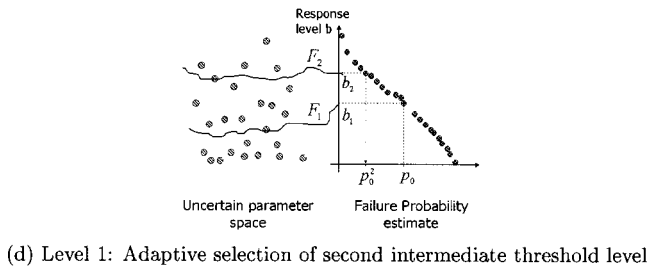
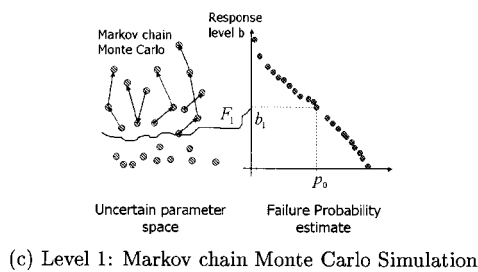
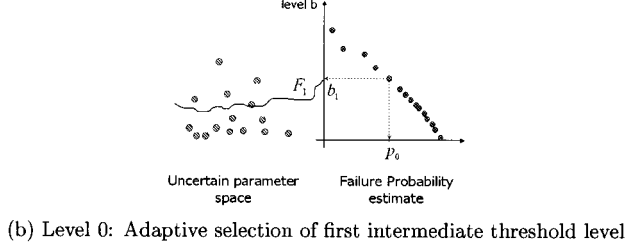
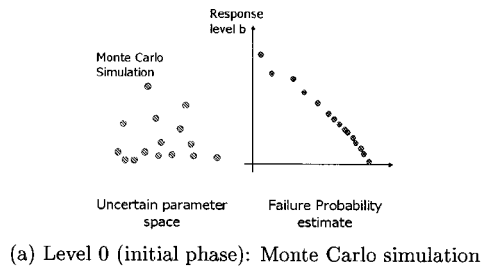


Fig. 2. Illustration of subset simulation procedure

positional PDF lies in how it can be chosen so that the candidate state has a distribution close to this conditional PDF in order that the simulation process is still efficient (with small correlation among Markov chain samples). Choosing an n -dimensional proposal PDF (i.e., with only one group of n uncertain parameters) will generally lead to “zero acceptance rate” of the precandidate state

when n is large (Au 2001; Au and Beck 2001a) and therefore grouping of the uncertain parameters is inevitable.

Note that the components of the candidate state corresponding to different groups are generated independently in Step 1. This is the key mechanism which makes the algorithm applicable even in high-dimensional problems (Au 2001; Au and Beck 2001a), but at the expense of implicitly enforcing independence among the uncertain parameters of different groups in the generation of the candidate state. If some uncertain parameters belonging to different groups are strongly correlated when conditional on the failure region, the distribution of the candidate state will not be close to the conditional PDF, at least in terms of the correlation structure among the uncertain parameters. Consequently, the acceptance rate with respect to the conditioning by F_i for the candidate state will be small. Thus, uncertain parameters that are strongly correlated with each other when conditional on F_i should be grouped together. In any case, the number of uncertain parameters in a group should be kept small to avoid high-dimensional problems.

Deciding what type of proposal PDF to use for a particular group depends on the role that the group of uncertain parameters has in affecting failure and on the information available for constructing the proposal PDF. Three types of groups are now discussed and are summarized in Table 1.

Type I: Insensitive Parameters

If failure is insensitive to a particular group of uncertain parameters, then the proposal PDF should be chosen as the original parameter PDF for that group, so that the precandidate component generated by the proposal PDF is always accepted into the candidate state in Step 1.

Type II: Large Number of Independent and Identically Distributed Uncertain Parameters

When there is a large number of uncertain parameters that all play a similar role in affecting failure, it often happens that these uncertain parameters as a whole affect failure significantly, but not individually. One common example is the set of i.i.d standard normal parameters in the discrete-time representation of Gaussian white noise in the first-excursion problem. In this case, each of these uncertain parameters should be grouped individually to avoid high-dimensional problems. For each uncertain parameter, one can choose a one-dimensional adaptive symmetric proposal PDF that is local to the current sample. The advantage of this choice is that a reasonable acceptance rate of the candidate state can often be guaranteed when the spread of the proposal PDF about the current sample is not too large, since then the corresponding components of the candidate state are generated in the

Table 1. Different Types of Proposal Probability Density Functions

Type	Description	Advantage	Disadvantage	Suitable for
I	Parameter probability density function, nonadaptive	100% acceptance in Step 1; precandidate component $\xi^{(j)}$ does not depend on current sample	Does not improve acceptance with respect to conditioning by F_i in Step 2	Insensitive parameters
II	One-dimensional chain-adaptive symmetric (Metropolis)	Good acceptance rate of candidate state without prior information on F_i	Correlation between current sample and candidate state may be high	Uncertain parameters which are abundant and influential as a group
III	n_j -D Metropolis-Hastings, chain-nonadaptive, level-adaptive	High-acceptance rate possible if uncertain parameters are influential, and conditional probability density function well approximated by proposal probability density function	Only for a small number of uncertain parameters	A small group of influential parameters

Table 2. Recommended Types of Proposal Probability Density Functions for Different Parameters in First-Excursion Problems ($\underline{\theta}_Z$ = Additive Excitation Parameters; $\underline{\theta}_E$ = Excitation Model Parameters)

Uncertain parameters in the problem	Type of proposal probability density function for	
	$\underline{\theta}_Z$	$\underline{\theta}_E$
$\underline{\theta}_Z$	II	
$\underline{\theta}_Z, \underline{\theta}_E$	I/II	III/II

neighborhood of those of the current sample. This choice of the proposal PDF will also cause the components of the candidate state to be positively correlated with those of the current sample, thereby slowing down convergence of the conditional failure probability estimate for the level, although this seems to be the best one can do in the absence of further prior knowledge about the failure region.

Type III: Small Number of Influential Uncertain Parameters

Consider the case where failure is sensitive to the uncertain parameters of a particular group. If there is some information about the failure region F_i so that a PDF can be constructed which is similar to the conditional PDF with respect to the uncertain parameters of this group, then such a PDF may be used as the proposal PDF, assuming that an efficient method is available for evaluating its value and for generating random samples according to it. The proposal PDF in this case is not “chain-adaptive,” in the sense that the distribution of the precandidate state component remains unchanged as the Markov chain develops. It plays a similar role to that of an importance sampling density with respect to the group of uncertain parameters. Similar methods to those for constructing importance sampling densities (ISDs) can be used for constructing the proposal PDF.

Regarding the information available for constructing the proposal PDF, it should be noted that the Markov chain samples from the last simulation level that lie in the failure region F_i are distributed as the conditional PDF $q(\cdot|F_i)$. In fact, they are used as the initial samples for starting individual Markov chains for the current simulation level. One way of utilizing these samples is to construct the proposal PDF as a normal PDF with mean and covariance matrix estimated from the samples. Another strategy is to construct the proposal PDF as a kernel sampling density using the samples (Silverman 1986; Ang et al. 1992; Au and Beck 1999). Since the information from the last simulation level is utilized to construct the proposal PDF at the current level, this choice is “level-adaptive.” It should be noted, however, that successful use of a level-adaptive proposal PDF is based on the premise that the conditional PDF with respect to the group of uncertain parameters can be approximated by the chosen type of PDF. Also, they should be used only when the number of uncertain parameters in the group is not large, for otherwise high-dimensional problems may occur as the number of members n_j in the group increases.

Group Types for First-Excursion Problems

For applications to solving the first-excursion problem, it is useful to group the uncertain parameters in the stochastic excitation model into two categories

1. Additive excitation parameters $\underline{\theta}_Z$; and
2. Stochastic excitation model parameters $\underline{\theta}_E$.

The first category includes the additive excitation parameters $\underline{\theta}_Z$ in the discrete representation of the stochastic excitation. The number of uncertain parameters in this category is often very large. For example, discretizing Gaussian white noise in the time domain of duration $T_d=30$ s and sampling time $\Delta t=0.02$ s requires $T_d/\Delta t+1=1,501$ i.i.d. standard normal random variables, assuming the time instants at time 0 and 30 s are both represented. These uncertain parameters are often influential as a group, but they are insensitive individually, because the dynamic response is affected by the “integral” (in continuous-time) or “summation” (in discrete-time) effect of these parameters, and the effect of each individual uncertain parameter on the response is infinitesimally small [e.g., $O(\Delta t)$ in discrete-time]. For this category of uncertain parameters, it is recommended that they be treated individually using a Type II proposal PDF.

The second category includes the stochastic excitation model parameters $\underline{\theta}_E$ involved in the stochastic excitation model, which often have a “multiplicative effect” on the response. Examples are the spectral intensity of white-noise excitation or the moment magnitude and epicentral distance in a stochastic ground motion point-source model. Due to their multiplicative effect and their large variability assumed in applications, these uncertain parameters often have a dominant effect on the uncertain response, rendering other uncertain parameters, such as those in $\underline{\theta}_Z$, less sensitive. Since these uncertain parameters control failure, their conditional distribution given failure is often significantly different from their parameter PDF. Capturing the conditional distribution of these uncertain parameters can lead to significant improvement in the efficiency of the simulation procedure, and hence a Type III proposal PDF is recommended, keeping in mind the requirement that the number of uncertain parameters in the group should be kept small to avoid high-dimensional problems. Table 2 summarizes the types of proposal PDFs recommended for the uncertain parameters of different categories in first-excursion problems.

Computational Efficiency

The computational efficiency for Subset Simulation relative to standard MCS increases with decreasing failure probability because the computational effort depends roughly on the logarithm of $P(F)$ and so grows more slowly as $P(F)$ decreases than for standard MCS. If the conditional failure regions are chosen so that the corresponding estimates of the conditional failure probabilities are all equal to p_0 (0.1 is recommended) and the same number of samples N is used in the simulation at each level, then from Eqs. (14) and (21), the c.o.v. of the estimator for a failure probability $P(F)=p_0^m$ (requiring m levels) is given by

$$\tilde{\delta}^2 = \frac{m(1-p_0)(1+\bar{\gamma})}{Np_0} \quad (26)$$

where $\bar{\gamma}$ = average value of the correlation parameters γ_i defined in Eq. (15) for the simulated samples at each level. The minimum number of samples required to give a c.o.v. of $\tilde{\delta}$ is therefore

$$N_T = mN = \frac{m^2(1-p_0)(1+\bar{\gamma})}{p_0\tilde{\delta}^2} \quad (27)$$

For standard MCS the minimum number of samples required to give a c.o.v. of $\tilde{\delta}$ is $N_0=(1-p_0^m)/p_0^m\tilde{\delta}^2$. A measure of the effi-

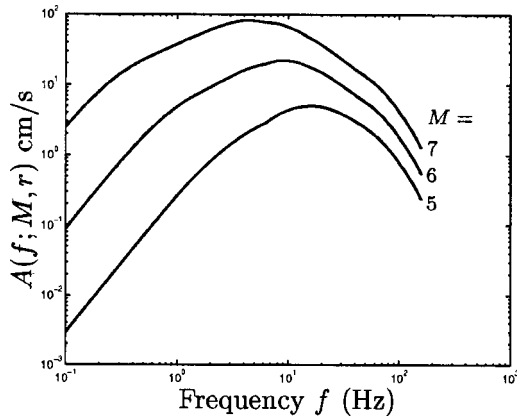


Fig. 3. Radiation spectrum $A(f; M, r)$ for $r=20$ km and $M=5,6,7$

ciency of Subset Simulation relative to standard MCS is then given by

$$\frac{N_0}{N_T} = \frac{1 - p_0^m}{m^2 p_0^{m-1} (1 - p_0)(1 + \bar{\gamma})} \quad (28)$$

It is noted that the computational overhead required for Subset Simulation, beyond that due to the system analysis for each sample that is also required in standard MCS, is negligible. Taking $p_0=0.1$, for $m=3$ and 6 that correspond to a target failure probability of $P(F)=10^{-3}$ and 10^{-6} , the above equation gives $N_0/N_T=4$ and $1,030$ (since $\bar{\gamma}$ is about 2). This shows that Subset Simulation becomes much more efficient than standard MCS for smaller values of $P(F)$. This gain in efficiency is based on $\bar{\gamma}$ not being large, which can be achieved if the proposal distribution is chosen properly.

Failure Analysis Using Markov Chain Samples

The Markov chain samples generated during Subset Simulation can be used not only for estimating the conditional probabilities but also to infer the probable scenarios that will occur in the case of failure. Essentially, they yield information for “failure analysis” to address the question: *What is expected to happen when the system fails?*

The distribution $q(\theta|F)$ of the uncertain parameters corresponding to the conditional samples for failure F gives an idea of the probable cause of failure should it occur. Also, the marginal PDF $q(\theta_i|F)$ for the uncertain parameter θ_i , when compared to marginal PDF $q(\theta_i)$ corresponding to the parameter PDF $q(\theta)$, shows how important the corresponding uncertain parameter θ_i is in affecting failure. In fact, by Bayes’ theorem, for a given value of θ_i

$$P(F|\theta_i) = \frac{q(\theta_i|F)}{q(\theta_i)} P(F) \quad (29)$$

and hence $P(F|\theta_i)$ will be insensitive to θ_i when the conditional PDF $q(\theta_i|F)$ is similar in shape to the PDF $q(\theta_i)$.

The distribution of some response quantity of interest, $h(\theta)$, evaluated at the Markov chain samples also gives information about the system performance when failure occurs. In particular, using the Markov chain samples $\{\theta_{i,k} : k=1, \dots, N\}$ conditional on the failure region F_i ($i=1, \dots, m$), the conditional expectation of $h(\theta)$ when the failure region F_i has occurred can be estimated by

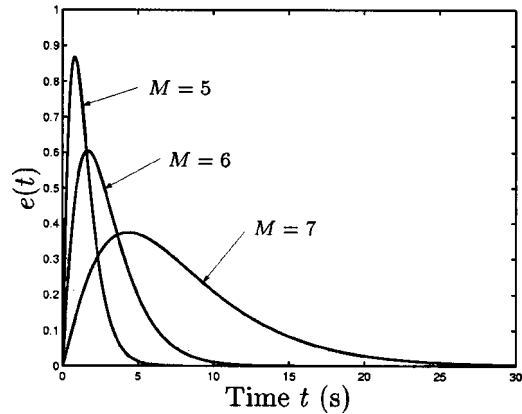


Fig. 4. Envelope function $e(t; M, r)$ for $r=20$ km and $M=5,6,7$

$$E[h(\theta)|F_i] = \int h(\theta)q(\theta|F_i)d\theta \approx \frac{1}{N} \sum_{k=1}^N h(\theta_{i,k}) \quad (30)$$

Applications to Seismic Risk Based on Dynamic Analysis

To illustrate the application of Subset Simulation to seismic risk, two structural systems are considered that are subjected to uncertain ground motions. The stochastic ground motion model and the seismic hazard are first described, then the results for the two structural systems are given.

Stochastic Ground Motion Model

The seismic risk problem is formulated using a stochastic ground motion model to describe the uncertainty associated with the ground motion at the site in a seismic event of given magnitude and earthquake source location. In this work, the stochastic ground motion model developed by Atkinson and Silva (2000) is adopted, which belongs to the class of point-source models characterized by the moment magnitude M and epicentral distance r (Brune 1971a,b; Hanks and McGuire 1981; Boore 1983). For easy reference, we will call this the A-S model. To generate a time history for the ground acceleration for given moment magnitude M and epicentral distance r , a discrete-time white noise sequence $\{W_j = \sqrt{2\pi}/\Delta t Z_j : j=1, \dots, n_t\}$ is first generated, where Z_1, \dots, Z_{n_t} are i.i.d. standard normal variables, and then it is modulated by an envelope function $e(t; M, r)$ at the

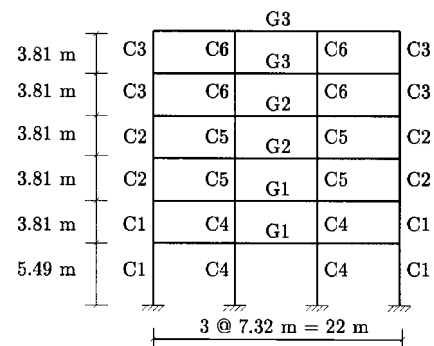


Fig. 5. Moment-resisting frame structure in Example 1

Table 3. Sections (AISC) for Frame Members in Example 1

Story	Exterior column	Interior column	Girder
1,2	C1: W14×159	C4: W27×161	G1: W24×94
3,4	C2: W14×132	C5: W27×114	G2: W24×76
5,6	C3: W14×99	C6: W24×84	G3: W24×55

discrete time instants. A discrete Fourier transform is then applied to the modulated white noise sequence. The resulting spectrum is multiplied with the “radiation spectrum” $A(f;M,r)$, after which the discrete inverse Fourier transform is applied to transform the sequence back to the time domain to yield a sample for the ground acceleration time history. The synthetic ground motion $a(t;Z,M,r)$ generated from the A-S model is thus a function of the additive excitation parameters $Z=[Z_1, \dots, Z_{n_r}]$ and the stochastic excitation model parameters M and r .

Radiation Spectrum

The A-S model is characterized by the radiation spectrum $A(f;M,r)$ and the envelope function $e(t;M,r)$. The radiation spectrum $A(f;M,r)$ consists of several factors which account for the spectral effects from the source as well as propagation through the earth crust. It is given by

$$A(f;M,r) = A_0(f)V(f) \frac{1}{R} \exp[-\gamma(f)R] \exp(-\pi f \kappa) \quad (31)$$

Here, A_0 is the “equivalent point-source spectrum” based on two corner frequencies, given by

$$A_0(f) = CM_o(2\pi f)^2 \left[\frac{1-\varepsilon}{1+(f/f_a)^2} + \frac{\varepsilon}{1+(f/f_b)^2} \right] \quad (32)$$

where M_o = seismic moment (in dyn-cm) given by (Kanamori 1977; Hanks and Kanamori 1979)

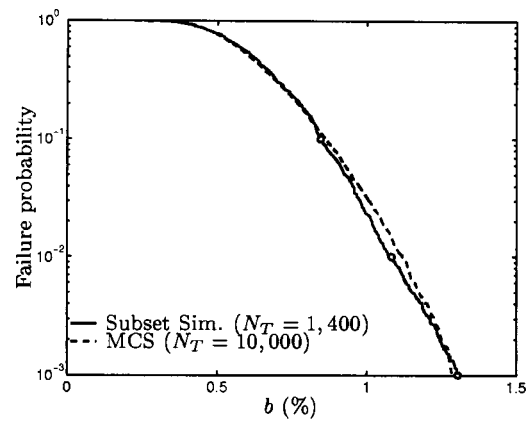
$$M_o = 10^{1.5(M+10.7)} \quad (33)$$

and $C = C_R C_P C_{FS} / (4\pi\rho\beta^3)$; $C_R = 0.55$ is the average radiation pattern coefficient (over all azimuths) for shear waves; $C_P = 1/\sqrt{2}$ is a coefficient to account for the partition of waves into two horizontal components; $C_{FS} = 2$ is the free surface amplification; ρ and β are the density and shear-wave velocity in the vicinity of the earthquake source, respectively, assumed to be 2.8 g/cm³ and 3.5 km/s. In Eq. (32), $f_a = 10^{2.18-0.496M}$ and $f_b = 10^{2.41-0.408M}$ are the lower and upper corner frequencies (in Hz) for the equivalent point-source spectrum, respectively. The parameter $\varepsilon = 10^{0.605-0.255M}$ is a weighting parameter.

In Eq. (31), $V(f)$ describes the amplification through the crustal velocity gradient as well as soil layers. Without detailed specification of the soil properties at the site, it is assumed that $V(f) = 2$, which lies in the range of values for NEHRP class C (corresponding to a mix of rock and soil sites) for frequencies

Table 4. Point Masses for Steel Frame in Example 1

Floor	Exterior column ($\times 10^3$ kg)	Interior column ($\times 10^3$ kg)
2	60.4	81.0
3	53.3	78.1
4	51.9	76.0
5	51.7	75.8
6	50.1	73.5
Roof	44.6	63.1

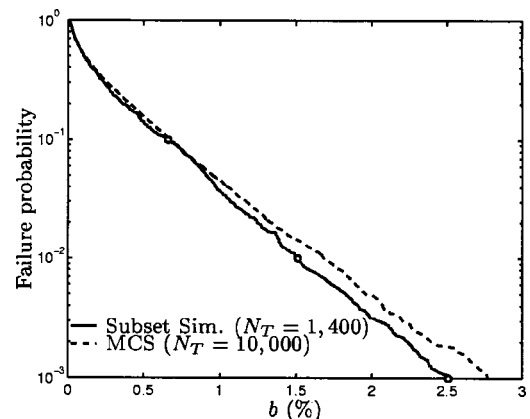
**Fig. 6.** Failure probability estimates for Example 1, Case 1

between 0.4 and 4 Hz (Boore and Joyner 1997). The term $1/R$ is the geometric spreading factor, where $R = \sqrt{h^2 + r^2}$ is the radial distance from the earthquake source to the site, r is the epicentral distance (in km), and h is the nominal depth of fault (in km). It is assumed that $h = 10^{-0.05+0.15M}$, which ranges from about 5 km at $M = 5$ to 14 km at $M = 8$. The term $\exp[-\gamma(f)R]$ in Eq. (31) accounts for an elastic attenuation, where $\gamma(f) = \pi f / Q\beta$ and $Q = 180f^{0.45}$ is a regional quality factor. The term $\exp(-\pi f \kappa)$ accounts for the near surface attenuation of high-frequency amplitudes, where κ is assumed to be 0.04.

Fig. 3 illustrates the dependence of the radiation spectrum on the moment magnitude for a nominal epicentral distance of $r = 20$ km. From Fig. 3, it can be seen that as the moment magnitude increases, the spectral amplitude in general increases at all frequencies, with a shift of dominant frequency content towards the lower-frequency regime, as expected. It should be noted that, roughly speaking, both M and r have a multiplicative effect on the synthetic ground acceleration $a(t;Z,M,r)$ and hence on the structural response. This observation implies that M and r are influential parameters for failure and so a Type III proposal PDF (Table 1) is chosen for them in the Subset Simulation.

Envelope Function

The envelope function $e(t;M,r)$ is the major factor affecting the duration of simulated ground motions for given M and r . It is assumed to be

**Fig. 7.** Failure probability estimates for Example 1, Case 2

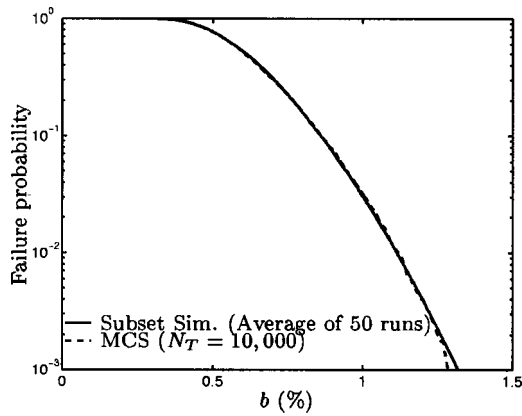


Fig. 8. Sample mean of failure probability estimates over 50 runs, Case 1

$$e(t;M,r) = c_3 t^{c_1} \exp(-c_2 t) U(t) \quad (34)$$

where $U(t)$ = unit-step function,

$$c_1 = - \frac{\varepsilon_1 \log \varepsilon_2}{1 + \varepsilon_1 (\log \varepsilon_1 - 1)} \quad (35)$$

$$c_2 = \frac{c_1}{\varepsilon_1 T_w} \quad (36)$$

and c_3 = normalizing factor, chosen to be

$$c_3 = \sqrt{\frac{(2c_2)^{2c_1+1}}{\Gamma(2c_1+1)}} \quad (37)$$

so that the envelope function has unit energy, in the sense that $\int_0^\infty e(t;M,r)^2 dt = 1$. Here, $\Gamma(\cdot)$ is the gamma function, and $T_w = 1/f_a + 0.1R$ is related to the duration of the envelope function. The parameters ε_1 and ε_2 are taken to be $\varepsilon_1 = 0.2$ and $\varepsilon_2 = 0.05$ (Boore 1983).

The envelope function $e(t;M,r)$ is shown in Fig. 4 for different magnitudes at $r = 20$ km. From Fig. 4, it can be seen that increasing the moment magnitude generally increases the duration of the envelope function, as expected.

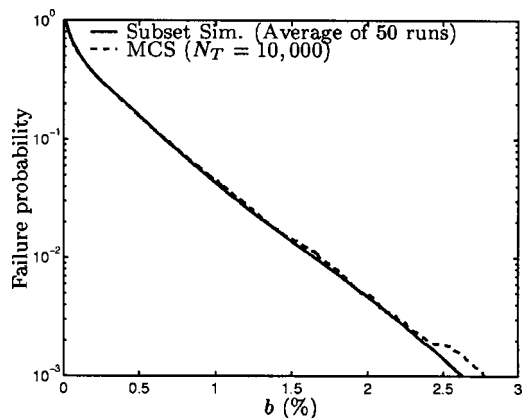


Fig. 9. Sample mean of failure probability estimates over 50 runs, Case 2

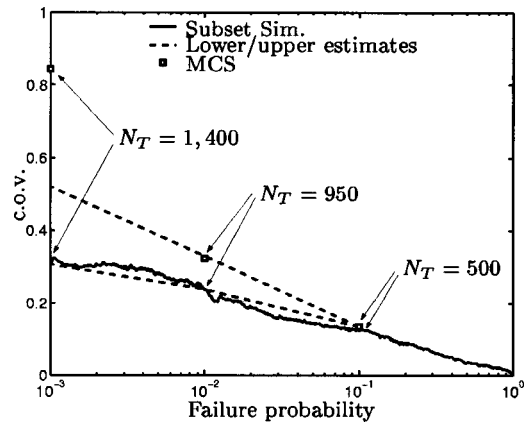


Fig. 10. Sample c.o.v. of failure probability estimates over 50 runs, Case 1

Choice of Seismic Hazard for Examples

For each structural example, two seismic hazard cases are considered: Case 1 is a large-event scenario and Case 2 is based on a probabilistic seismic hazard that explicitly considers the uncertain regional seismicity. In both cases, the A-S model is used to generate a synthetic ground acceleration $a(t;Z,M,r)$ for given M and r , where $Z = [Z_1, \dots, Z_{n_t}]$ is a standard normal vector and n_t is the number of time instants. In Case 2, where the regional seismic hazard is considered, the uncertainty in M and r also has to be addressed. The time step and duration of interest are taken to be 0.02 and 30 s, respectively, for both the simulation of ground motions and the dynamic structural analyses. The number of additive excitation parameters Z involved in the generation of ground motion for a given stochastic model is thus $n_t = 30/0.02 + 1 = 1501$, where the time instants at $t = 0$ and $t = 30$ are also represented.

Case 1: Large-Event Scenario

In Case 1, only the additive excitation parameters $Z = [Z_1, \dots, Z_{n_t}]$ for generating the ground motion $a(t;Z,M,r)$ are assumed to be uncertain; the moment magnitude M and epicentral distance r are fixed at the values: $M = 7$ and $r = 20$ km.

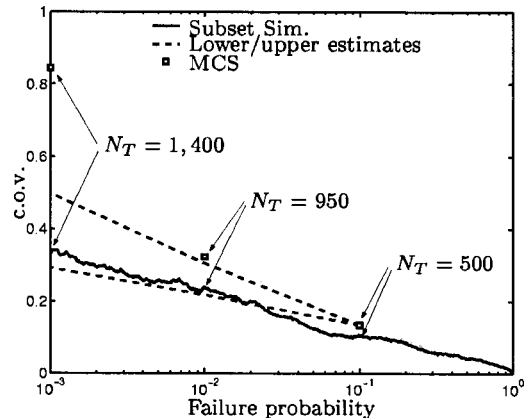


Fig. 11. Sample c.o.v. of failure probability estimates over 50 runs, Case 2

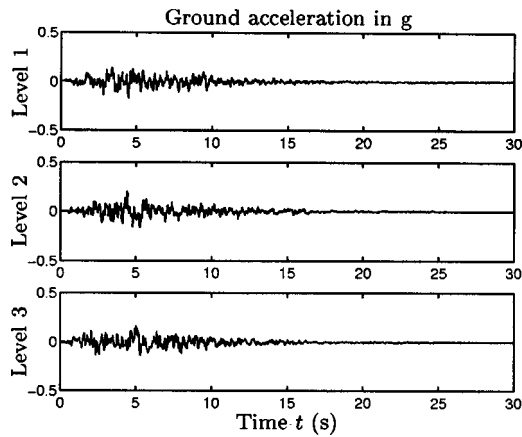


Fig. 12. Ground motions for Example 1, Case 1, conditional levels 1,2,3

This case corresponds to the classical first-excursion problem with a given stochastic excitation model defined by fixed M and r .

Case 2: Uncertain Regional Seismicity

In Case 2, in addition to the uncertain additive excitations, M and r are also considered to be uncertain with specified probability distributions. This corresponds to a full seismic risk problem where the uncertainty in the regional seismicity is also addressed.

In the examples, the uncertainty in the moment magnitude is modeled by the Gutenberg-Richter relationship, truncated on the interval $[M_{\min}, M_{\max}]$ (Gutenberg and Richter 1958; Kramer 1996)

$$q(M) = \frac{\beta' \exp(-\beta' M)}{\exp(-\beta' M_{\min}) - \exp(-\beta' M_{\max})}, \quad M_{\min} \leq M \leq M_{\max} \quad (38)$$

where $\beta' = b \log_e(10)$ and $b =$ coefficient appearing in the annual relative frequency (λ_M) description of the number of earthquakes with magnitude up to M : $\lambda_M = 10^{a-bM}$. It is assumed that $M_{\min} = 5$, $M_{\max} = 8$, $b = 1$.

For the uncertainty in event location, earthquakes of magnitude between M_{\min} and M_{\max} are assumed to occur equally likely in a circular area of radius $r_{\max} = 50$ km centered at the site where

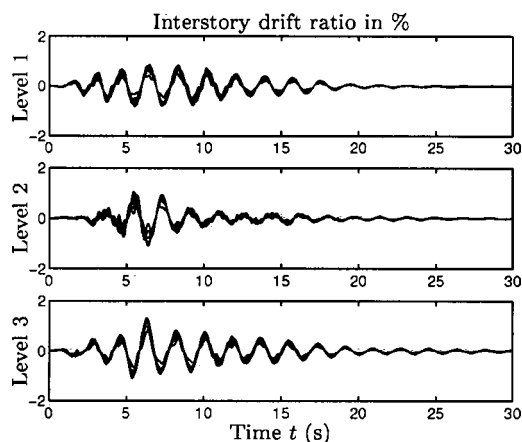


Fig. 13. Response of all stories, Case 1, conditional levels 1,2,3

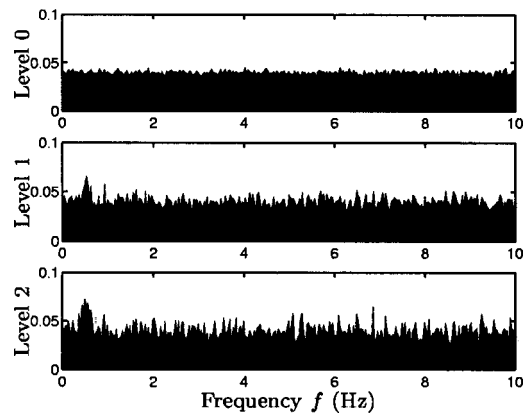


Fig. 14. Spectra of white noise sequence, Case 1, conditional levels 0,1,2

the structure is situated. This leads to a triangular distribution for the epicentral distance r confined to the interval $[0, r_{\max}]$

$$q(r) = \begin{cases} 2r/r_{\max}^2 & r \in [0, r_{\max}] \\ 0 & \text{otherwise} \end{cases} \quad (39)$$

Subset Simulation Parameters

In the application of Subset Simulation in the examples, the conditional failure regions are chosen such that a conditional failure probability of $p_0 = 0.1$ is attained at all simulation levels. At each simulation level, $N = 500$ samples are simulated. Failure probabilities ranging from 10^{-3} to 1 will be estimated, or in other words, the response level corresponding to failure probabilities as small as 10^{-3} will be estimated. The total number of samples required to produce the failure probability versus threshold level curve is thus $N_T = 500 + 450 + 450 = 1400$, because 50 failure events from one level are used to start the next higher level and so only a further 450 samples are required for that level.

For the additive excitation $\underline{Z} = [Z_1, \dots, Z_n]$, each Z_i is grouped as a single component, for which the proposal PDF is chosen as a one-dimensional (chain-adaptive) symmetric uniform distribution (Type II in Table 1) with maximum step length $l_i = 1$, that is, $p^*(\xi_i | \theta_i) = 1/2$ if $|\xi_i - \theta_i| \leq 1$ and 0 otherwise. For the stochastic excitation model parameters, M and r , a level-

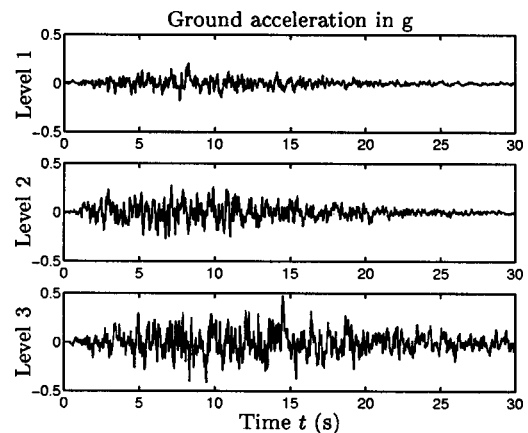


Fig. 15. Ground motions for Example 1, Case 2, conditional levels 1,2,3

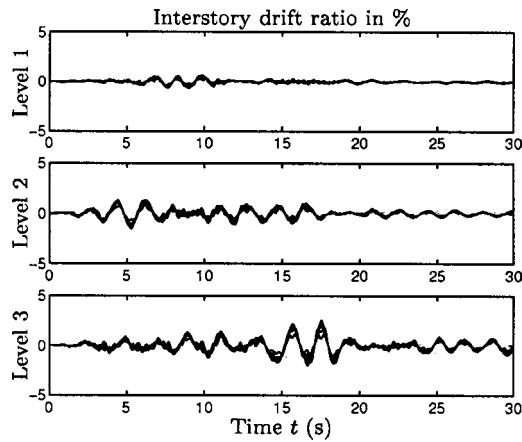


Fig. 16. Response of all stories, Case 2, conditional levels 1,2,3

adaptive proposal PDF (Type III in Table 1) is used, which is constructed as a kernel sampling density using the Markov chain samples from the last simulation level.

Example 1: Linear Moment-Resisting Steel Frame

Consider a six-story moment-resisting steel frame as shown in Fig. 5 with member sections given in Table 3. For each floor, the same section is used for all girders. The structure is modeled as a two-dimensional linear frame with beam elements connecting the joints of the frame. Masses are lumped at the nodes of the frame, which include the contributions from the dead load of the floors and the frame members. They are tabulated in Table 4. The natural frequencies of the first two modes are computed to be 0.552 and 1.56 Hz, respectively. Rayleigh damping is assumed so that the first two modes have 5% of critical damping. Failure is defined as the exceedance of a specified interstory drift ratio b at any one of the (twenty four) columns within the duration of interest (30 s). (The columns within a story experience essentially the same drift).

Failure Probability Estimation

Figs. 6 and 7 show the estimates of failure probability for different threshold levels b for Cases 1 and 2, respectively. Note that a total of $N_T=1,400$ samples, i.e., dynamic structural analyses, are

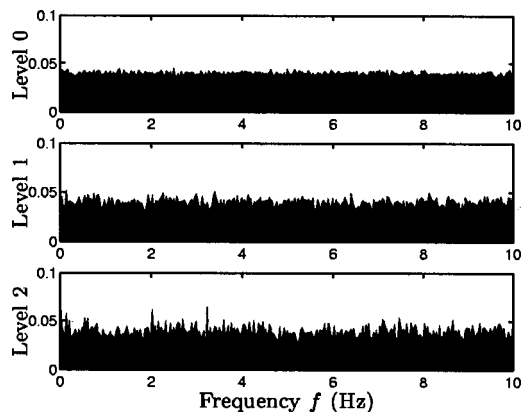


Fig. 17. Spectra of white noise sequence, Case 2, conditional levels 0,1,2

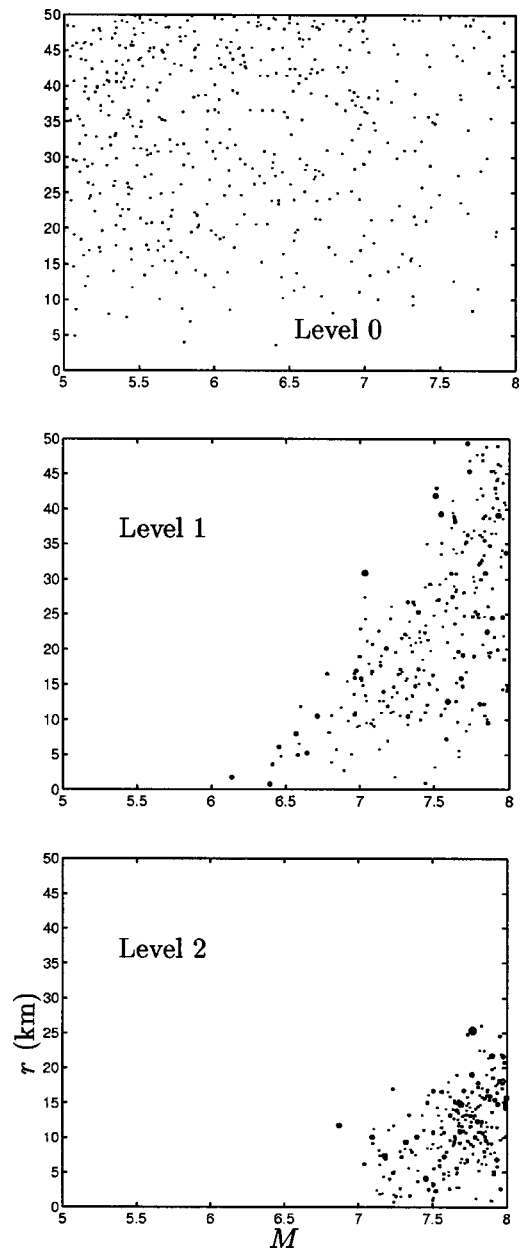


Fig. 18. Conditional samples of M and r for Example 1, Case 2, at conditional levels 0,1,2

performed to compute the results (solid line) in each figure. The results computed by standard Monte Carlo simulation (MCS) with 10,000 samples (so that the c.o.v. at a failure probability of 10^{-3} is about 30%) is also shown in the figures for comparison. These figures give an idea of how the results computed using Subset Simulation in a single run approximate the “exact” failure probabilities (of MCS).

To assess quantitatively the statistical properties of the failure probability estimates produced by Subset Simulation, 50 independent runs are carried out and the sample mean and sample c.o.v. of the failure probability estimates are computed. The results for the sample mean for the seismic hazard of Cases 1 and 2 are shown in Figs. 8 and 9, respectively. These figures show that the sample mean of the failure probability estimates are generally close to the results computed by standard Monte Carlo simulation, except for small failure probabilities near 10^{-3} where the results by MCS are inaccurate due to the number of samples used.

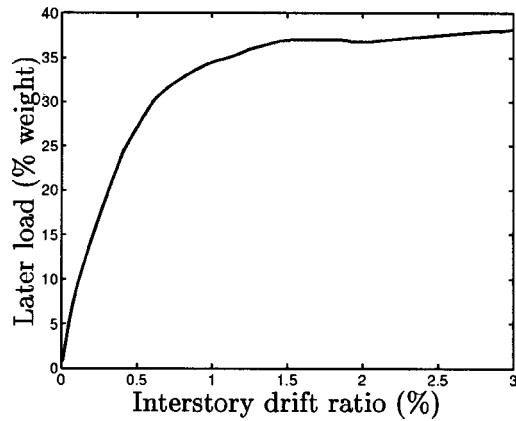


Fig. 19. Pushover curve for structure in Example 2

It can be concluded from the figures that the failure probability estimates by Subset Simulation are practically unbiased.

The sample c.o.v. for the failure probability estimates are shown in Figs. 10 and 11. The results are plotted versus different failure probability levels. The average results for the estimates of c.o.v. based on Eqs. (20) and (21) are also shown in the figures. Recall that Eq. (20) is an upper bound on the c.o.v. that assumes full correlation among the conditional failure probabilities at different simulation levels, while Eq. (21) assumes that they are independent. From Figs. 10 and 11, it can be seen that the trend in the actual c.o.v. estimated from the 50 runs follows more closely the lower estimate based on Eq. (21), suggesting that this formula can be used to assess the c.o.v. of the failure probability estimate in a single run.

The computational efficiency of Subset Simulation is next compared with that of standard Monte Carlo simulation in terms of the c.o.v. of failure probability estimates computed from the same number of samples. Note that the number of samples required by Subset Simulation at the probability levels $P(F) = 10^{-1}, 10^{-2}, 10^{-3}$ are $N_T = 500, 950, 1,400$, respectively. Using $\delta = \sqrt{[1 - P(F)]/P(F)N_T}$, the c.o.v. of the Monte Carlo estimator using the same number of samples at probability levels $10^{-1}, 10^{-2}$, and 10^{-3} are computed to be 0.13, 0.32, and 0.84, respectively, which are also shown as squares in Figs. 10 and 11. These figures show that as the failure probability decreases, the c.o.v. of the Monte Carlo estimator increases rapidly, while the c.o.v. of Subset Simulation increases at a much slower rate. This shows

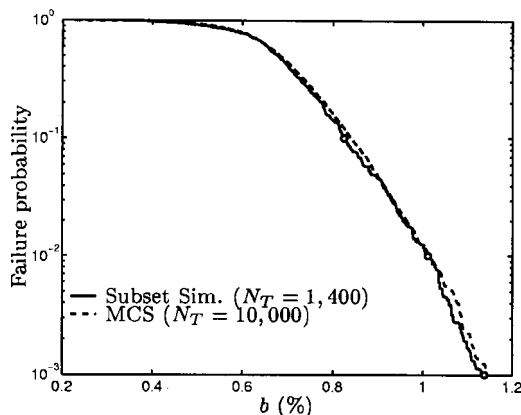


Fig. 20. Failure probability estimates for Example 2, Case 1

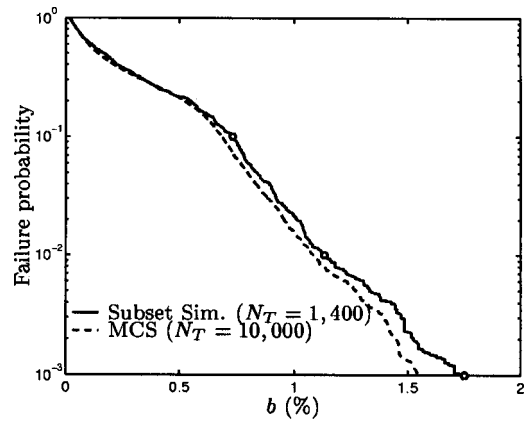


Fig. 21. Failure probability estimates for Example 2, Case 2

that Subset Simulation can lead to a substantial improvement in efficiency over standard Monte Carlo simulation when estimating small failure probabilities.

Failure Analysis Using Conditional Samples

The Markov chain samples at the different failure levels simulated in a single run of Subset Simulation are next examined for the purpose of failure analysis. Fig. 12 shows the typical samples of ground acceleration $a(t; Z, M, r)$ that correspond to failure probabilities $10^{-1}, 10^{-2}$, and 10^{-3} (failure levels 1, 2, and 3, respectively) for Case 1. Note that only the additive excitation parameters Z are uncertain in this case. The interstory drift response of all stories corresponding to these ground excitations are shown in Fig. 13. Since samples of acceleration time histories are generated for given moment magnitude $M = 7$ and epicentral distance $r = 20$ km, there is not much difference in their duration as well as mean square values. In terms of peak acceleration, they do not differ significantly, either. The major difference among these samples of ground acceleration that lead to different levels of failure lies in the frequency content. Fig. 14 shows the average spectrum (power spectral density) of the additive excitation parameters Z corresponding to the 500 samples of acceleration time histories at different levels of failure. Here, Level 0 refers to the initial phase of Subset Simulation where samples are generated directly from their parameter PDF, that is, standard Monte Carlo simulation.

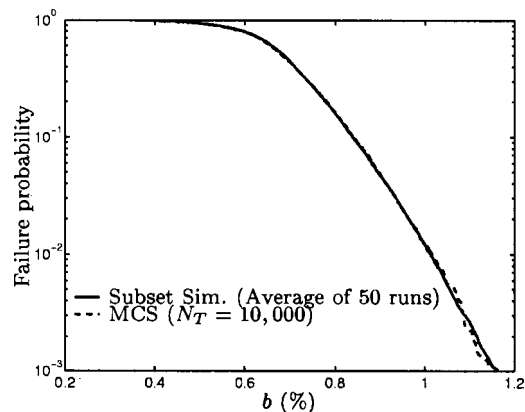


Fig. 22. Sample mean of failure probability estimates over 50 runs, Case 1

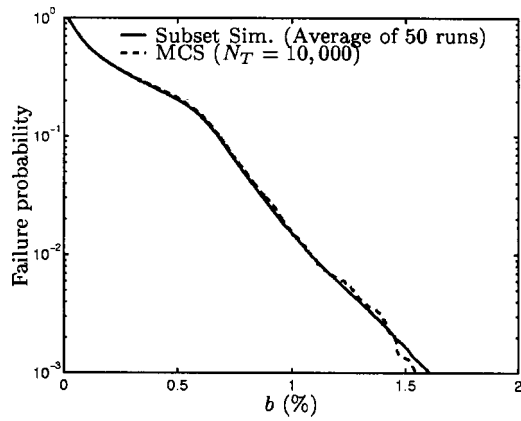


Fig. 23. Sample mean of failure probability estimates over 50 runs, Case 2

The spectrum at Level 0 (top plot of Fig. 14) is almost flat, because there is no conditioning on the samples at this level and therefore the spectrum theoretically corresponds to that of white noise, which is flat up to the Nyquist frequency, being $1/2\Delta t = 25$ Hz. As the simulation level increases, the spectrum develops a peak near 0.55 Hz, which is the natural frequency of the structure. This illustrates an important statistical feature of the additive excitations that lead to failure in the classical first-excursion problem (with deterministic structure and stochastic excitation model): *The additive excitation tends to “tune” itself to the natural frequency of the structure to cause first-excursion failure.* In other words, when the stochastic excitation model parameters are fixed, the probable cause of failure for the structure is due to resonance effects, especially when the threshold level is high.

This phenomenon can be explained as follows. The probability of a particular excitation decreases exponentially with the square of its Euclidean norm (energy). When the stochastic excitation model, and hence the excitation intensity, is fixed, it is not probable that the excitation will have a significantly large energy (e.g., in terms of mean square value) when failure occurs, since this will mean that the vector of additive excitation parameters \underline{Z} will have an Euclidean norm in the n_r -dimensional standard normal space significantly larger than other “typical” configurations. Rather, a more probable configuration for \underline{Z} to cause failure is to have its components “tuned” so that they have a frequency con-

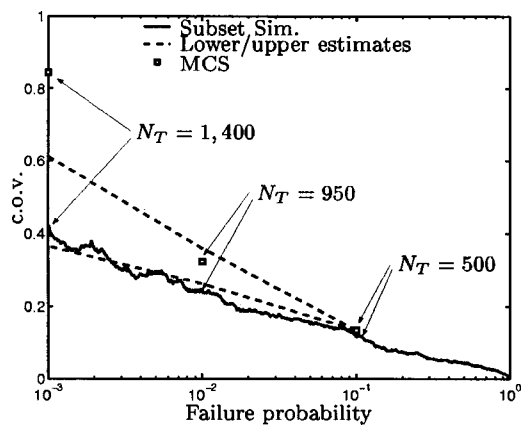


Fig. 24. Sample c.o.v. of failure probability estimates over 50 runs, Case 1

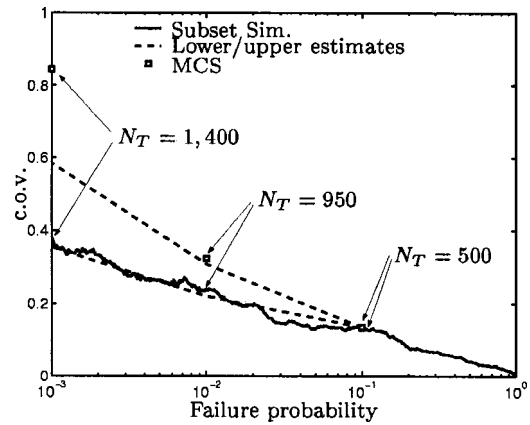


Fig. 25. Sample c.o.v. of failure probability estimates over 50 runs, Case 2

tent near the natural frequency of the structure to create a resonance effect, while the Euclidean norm of the whole vector \underline{Z} still remains more or less the same.

The situation is different when the stochastic excitation model parameters, M and r , are also uncertain. Figs. 15, 16, and 17 show the conditional samples and the average spectra at different simulation levels for Case 2, where \underline{Z} , M , and r are considered uncertain in the problem. Fig. 15 shows that in this case the excitation intensity and duration of the ground acceleration differ significantly at different simulation levels. Both the excitation intensity and duration increase as the simulation level increases. From Fig. 17, it can be seen that the spectral peak at 0.55 Hz for Levels 2 and 3 is not as significant as observed in Case 1 (Fig. 14). This indicates that the frequency content of the additive excitation \underline{Z} when failure occurs is not significantly different from its original spectrum (flat), although this does not imply that the frequency content of the ground acceleration will be the same irrespective of whether failure occurs, since the radiation spectrum $A(f;M,r)$ could be different because of the change in the distribution of M and r when failure occurs.

When the moment magnitude M and the epicentral distance r are uncertain, they are the parameters that control failure. Fig. 18 shows the scattering of samples of (M, r) at different levels. Note that the samples of (M, r) at Level 0 are simulated according to their PDF. Also, for Levels 1 and 2, some of the locations shown

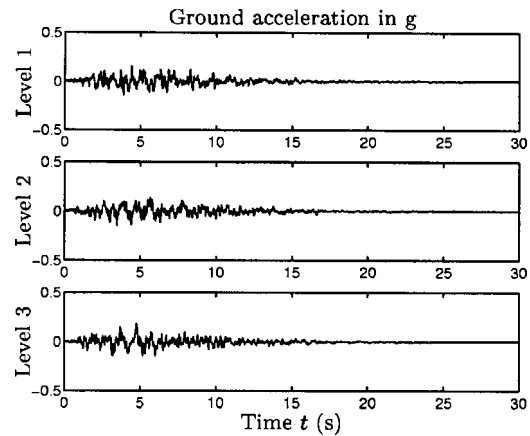


Fig. 26. Ground motions for Example 2, Case 1, conditional levels 1,2,3

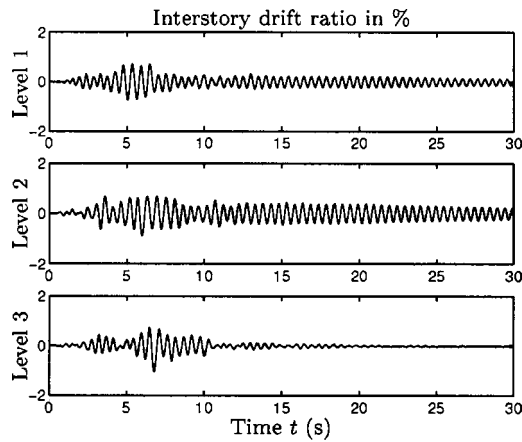


Fig. 27. Response, Case 1, conditional levels 1,2,3

in the figure contain repeated samples. Since the Markov chain samples are not all distinct, to show the population of the samples consistently, the dots are shown with area proportional to the number of points situated at the particular location. Fig. 18 clearly indicates that as the simulation level increases, that is, when failure becomes more severe, the samples of (M,r) shift towards the “large magnitude, small distance” regime.

Example 2: Nonlinear Concrete Portal Frame

The structural model in this example is a nonlinear concrete portal frame. It corresponds to Example 3 of the illustrative examples for the nonlinear finite element software OpenSees developed at the PEER (Pacific Earthquake Engineering Research) Center. The finite element model of the structure and its detailed description can be obtained from the website (<http://opensees.berkeley.edu/OpenSees/examples.html>). The general properties of the structural model are briefly described here. The frame is 3.66 m high by 9.15 m wide. An elastic beam element is used to model the beam connecting the two columns. The reinforced concrete section of the columns are modeled using steel and concrete fibers. The section of each column is 61 cm (24 in.) by 38 cm (15 in.) wide, with its strong axis perpendicular to the frame, that is, the columns deform in their strong direction during in-plane motion. The section is divided into confined and unconfined concrete regions, for which the fibers are discretized separately. The Kent-Scott-

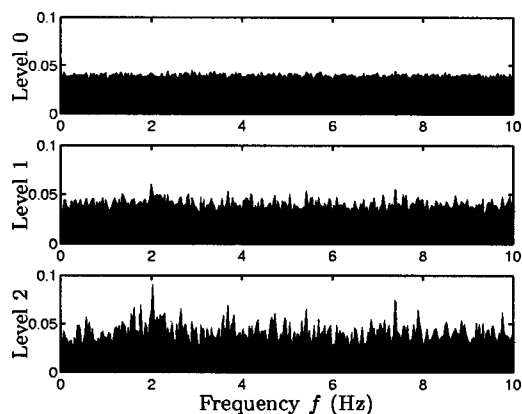


Fig. 28. Spectra of white noise sequence, Case 1, conditional levels 0,1,2

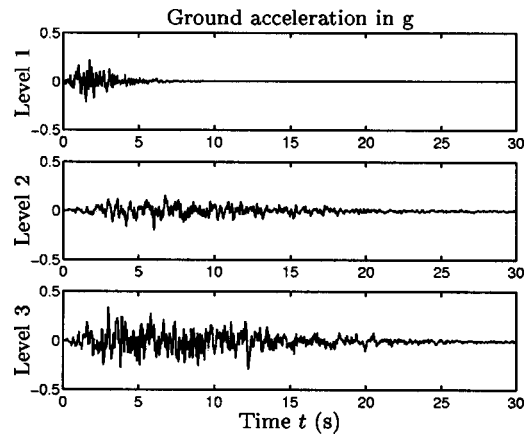


Fig. 29. Ground motions for Example 2, Case 2, conditional levels 1,2,3

Park model (Kent and Park 1971) is used for modeling the concrete material, with degraded linear unloading/reloading according to the work of Karsan and Jirsa (1969). Reinforcing steel bars are placed around the interface boundary of the confined and unconfined concrete regions. The reinforcing steel is modeled as a bilinear material with kinematic hardening.

The gravity load consists of two point loads of 801 kN (180 kips) at each of the columns. Fig. 19 shows a pushover curve of the structure. The small-amplitude natural frequency of the structure is 2.6 Hz. Viscous damping is included with the damping ratio for the first mode of vibration at small amplitudes being approximately 0.5%. Additional hysteretic damping develops in the structure during vibration at higher amplitudes.

Failure Probability Estimation

Failure is defined as the exceedance of a specified story drift ratio b . Figs. 20 and 21 show the estimates of failure probability for different threshold levels b for Cases 1 and 2, respectively. The sample mean of failure probability estimates over 50 independent simulation runs for Cases 1 and 2 are shown in Figs. 22 and 23, respectively. These figures show that the failure probability estimates by Subset Simulation are practically unbiased. The sample c.o.v. for the failure probability estimates computed using 50 independent simulation runs are shown in Figs. 24 and 25. In gen-

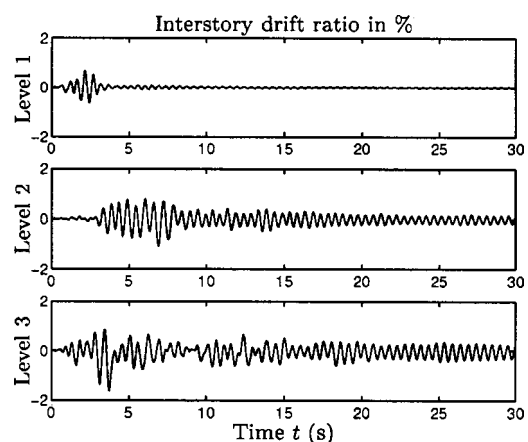


Fig. 30. Response, Case 2, conditional levels 1,2,3

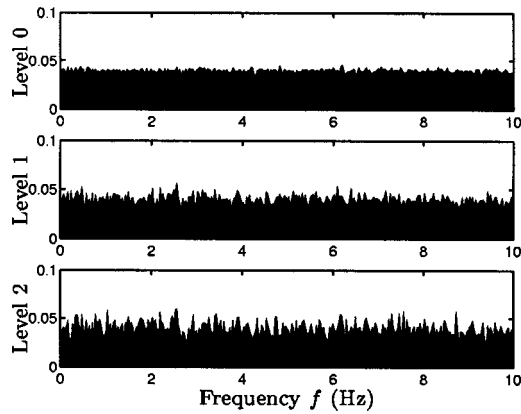


Fig. 31. Spectra of white noise sequence, Case 2, conditional levels 0,1,2

eral, it is observed that the performance of Subset Simulation in the current example for a nonlinear structure is similar to Example 1 for a linear structure, showing that the performance of Subset Simulation is robust to the type of structural model assumed in the analysis.

The trend of the failure probability versus threshold level b shown in Fig. 23 for Example 2 is qualitatively different from that in Fig. 9 for Example 1. In particular, in Example 2 (Fig. 23), the decay rate of failure probability with increasing threshold level b increases at around $b=0.5\%$. This is due to hysteretic damping which starts to become important at an interstory drift ratio of 0.5% where significant yielding occurs. The stiffness-softening of the structure in Example 2 starts to become dominant and outweighs the hysteretic damping effect at a drift ratio of around 1%, at which point the decay rate decreases.

Failure Analysis Using Conditional Samples

Fig. 26 shows the typical samples of ground acceleration that correspond to different levels of failure with failure probabilities 10^{-1} , 10^{-2} , and 10^{-3} for Case 1, where only the additive excitations \underline{Z} are uncertain. The interstory drift ratio of the left column (which is essentially the same as that of the right column) corresponding to these ground excitations is shown in Fig. 27. Fig. 28 shows the average spectrum of the additive excitation \underline{Z} at different levels of failure. As the simulation level increases, the spectrum develops a peak near 2 Hz, which is near the natural frequency of the structure (2.6 Hz). These observations are similar to those in Example 1. Nevertheless, the spectral peak in this case is less distinct and does not occur at the small-amplitude natural frequency of the structure. This is presumably due to the softening behavior of the structure at large amplitudes of vibration, which results in an apparently smaller “resonance frequency” adapted by the Markov chain samples of the additive excitation.

The system behavior for Case 2 of Example 2 is essentially similar to that of Example 1, as shown in Figs. 29, 30, 31, and 32.

Conclusions

Subset Simulation (Au and Beck 2001a) utilized in this study is based on (1) the representation of small failure probabilities as a product of larger conditional failure probabilities; and (2) Markov chain Monte Carlo (MCMC) simulation to efficiently generate samples conditional on intermediate failure regions. The im-

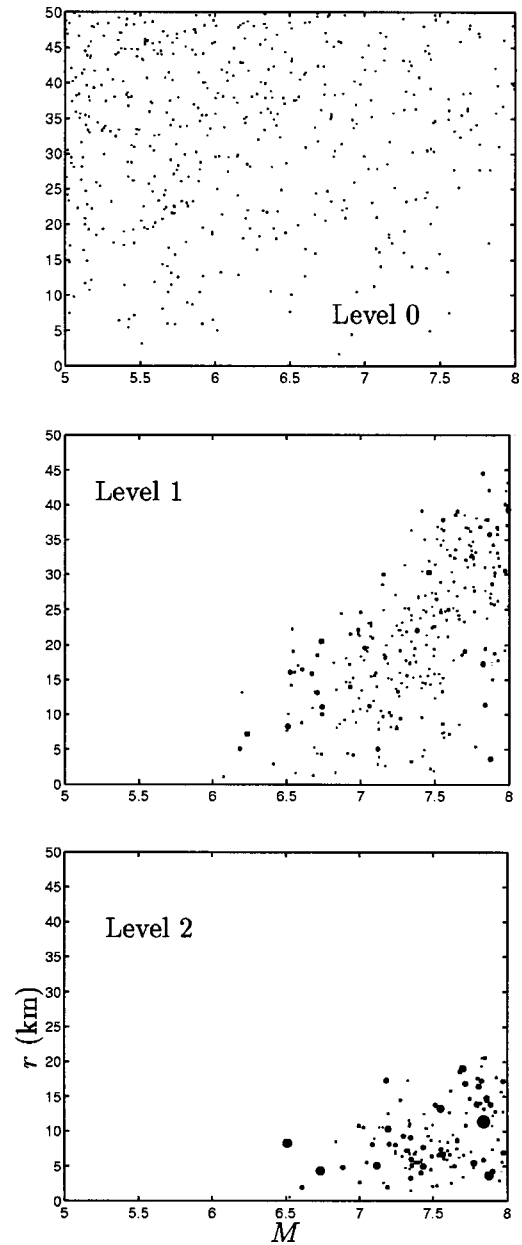


Fig. 32. Conditional samples of M and r for Example 2, Case 2, at conditional levels 0,1,2

proved MCMC algorithm presented in this paper allows greater flexibility for incorporating prior information about the problem in the simulation procedure so as to improve efficiency of the method. During Subset Simulation, the Markov chain samples are gradually adapted to failure regions of small failure probabilities. In addition to estimating failure probability, the Markov chain samples can also be used for failure analysis, which yields information about the probable scenario that will occur in a failure event.

The applicability and efficiency of Subset Simulation for computing the failure probabilities of structures during seismic risk studies using dynamic analysis have been demonstrated for both linear and nonlinear hysteretic models of structures. Failure analysis has been carried out using the samples generated during Subset Simulation to gain insight into the system behavior when failure occurs. The analysis shows that when only the seismic ground acceleration time history is uncertain, the rare failure sce-

narios correspond to resonance of the excitation with the structure. On the other hand, when the earthquake magnitude M and epicentral distance r defining the stochastic excitation model are also uncertain, they tend to control failure, due to their multiplicative effects on the response. The conditional distribution of M and r given that failure occurs is significantly different from their original PDF.

It should be noted that the observations from the failure analysis, such as the distribution of the moment magnitudes and epicentral distance when failure occurs, are based on the assumed probability models for the ground acceleration. The results should be interpreted bearing in mind the inherent limitations of these models. For example, the Atkinson-Silva model used in this study is a point-source model that does not directly account for the geometry of the fault and the characteristics of near-source ground motions. Nevertheless, on the premise that the quality of stochastic ground motion models will continue to improve, Subset Simulation provides a useful tool for seismic performance assessment through efficient estimation of failure probabilities and studies of failure analysis behavior based on dynamic analysis.

Acknowledgments

This paper was based upon work partly supported by the Pacific Earthquake Engineering Research Center under the National Science Foundation Cooperative Agreement No. CMS-9701568. This support is gratefully acknowledged. Part of this work was prepared when the first writer was at graduate standing at the California Institute of Technology, whose generous financial support is gratefully acknowledged.

References

- Ang, G. L., Ang, A. H.-S., and Tang, W. H. (1992). "Optimal importance-sampling density estimator." *J. Eng. Mech.*, 118(6), 1146–1163.
- Atkinson, G. M., and Silva, W. (2000). "Stochastic modeling of California ground motions." *Bull. Seismol. Soc. Am.*, 90(2), 255–274.
- Au, S. K. (2001). "On the solution of first excursion problems by simulation with applications to probabilistic seismic performance assessment." PhD thesis in Civil Engineering, *EERL Rep. No. 2001-02*, California Institute of Technology, Pasadena, Calif., available at <http://www.ntu.edu.sg/home/ckskau>.
- Au, S. K., and Beck, J. L. (1999). "A new adaptive importance sampling scheme." *Struct. Safety*, 21, 135–158.
- Au, S. K., and Beck, J. L. (2001a). "Estimation of small failure probabilities in high dimensions by subset simulation." *Probab. Eng. Mech.*, 16(4), 263–277.
- Au, S. K., and Beck, J. L. (2001b). "First-excursion probabilities for linear systems by very efficient importance sampling." *Probab. Eng. Mech.*, 16, 193–207. Software available at <http://www.ntu.edu.sg/home/ckskau>.
- Au, S. K., and Beck, J. L. (2002). "Importance sampling in high dimensions." *Struct. Safety*, 25(2), 139–163.
- Au, S. K., Papadimitriou, C., and Beck, J. L. (1999). "Reliability of uncertain dynamical systems with multiple design points." *Struct. Safety*, 21, 113–133.
- Beck, J. L., and Au, S. K. (2002). "Bayesian updating of structural models and reliability using Markov Chain Monte Carlo simulation." *J. Eng. Mech.*, 128(4), 380–391.
- Boore, D. M. (1983). "Stochastic simulation of high-frequency ground motions based on seismological models of the radiated spectra." *Bull. Seismol. Soc. Am.*, 73(6), 1865–1894.
- Boore, D. M., and Joyner, W. B. (1997). "Site amplifications for generic rock sites." *Bull. Seismol. Soc. Am.*, 87(2), 327–341.
- Brune, J. N. (1971a). "Correction." *J. Geophys. Res.*, 76, 5002.
- Brune, J. N. (1971b). "Tectonic stress and spectra of seismic shear waves from earthquakes." *J. Geophys. Res.*, 75, 4997–5009.
- Bucher, C. G. (1988). "Adaptive sampling—An iterative fast Monte Carlo procedure." *Struct. Safety*, 5, 119–126.
- Cornell, C. A. (1996). "Reliability-based earthquake-resistant design: the future." *Proc., 11th World Conf. on Earthquake Engineering*, International Association of Earthquake Engineering, Acapulco, Mexico.
- Cox, R. T. (1961). *The algebra of probable inference*, Johns Hopkins, Baltimore.
- Der Kiureghian, A., and Dakessian, T. (1998). "Multiple design points in first and second-order reliability." *Struct. Safety*, 20, 37–49.
- Engelund, S., and Rackwitz, R. (1993). "A benchmark study on importance sampling techniques in structural reliability." *Struct. Safety*, 12, 255–276.
- Fishman, G. S. (1996). *Monte Carlo: Concepts, algorithms, and applications*, Springer-Verlag, New York.
- Freudenthal, A. M. (1947). "The safety of structures." *Trans. Am. Soc. Civ. Eng.*, 112, 125–180.
- Freudenthal, A. M. (1956). "Safety and the probability of structural failure." *Trans. Am. Soc. Civ. Eng.*, 121, 1337–1397.
- Freudenthal, A. M., Garrelts, J. M., and Shinozuka, M. (1966). "The analysis of structural safety." *J. Struct. Div., ASCE*, 92(1), 267–325.
- Gutenberg, B., and Richter, C. (1958). "Earthquake magnitude, intensity and acceleration." *Bull. Seismol. Soc. Am.*, 62(2), 105–145.
- Hammersley, J. M., and Handscomb, D. C. (1964). *Monte-Carlo methods*, Methuen, London.
- Hanks, T. C., and Kanamori, H. (1979). "A moment magnitude scale." *J. Geophys. Res. B*, 84, 2348–2350.
- Hanks, T. C., and McGuire, R. K. (1981). "The character of high-frequency of strong ground motion." *Bull. Seismol. Soc. Am.*, 71(6), 2071–2095.
- Hastings, W. K. (1970). "Monte Carlo sampling methods using Markov chains and their applications." *Biometrika*, 57, 97–109.
- Kanamori, H. (1977). "The energy release in great earthquakes." *J. Geophys. Res.*, 82, 2981–2987.
- Karsan, I. D., and Jirsa, J. O. (1969). "Behavior of concrete under compressive loadings." *J. Struct. Div., ASCE*, 95(12), 2543–2563.
- Kent, D. C., and Park, R. (1971). "Flexural members with confined concrete." *J. Struct. Div., ASCE*, 97(7), 1969–1990.
- Kramer, S. L. (1996). *Geotechnical earthquake engineering*, Prentice-Hall, Englewood Cliffs, New Jersey.
- Melchers, R. E. (1989). "Importance sampling in structural systems." *Struct. Safety*, 6, 3–10.
- Metropolis, N., Rosenbluth, A. W., Rosenbluth, M. N., and Teller, A. H. (1953). "Equations of state calculations by fast computing machines." *J. Chem. Phys.*, 21(6), 1087–1092.
- Papadimitriou, C., Beck, J. L., and Katafygiotis, L. S. (1997). "Asymptotic expansions for reliabilities and moments of uncertain dynamic systems." *J. Eng. Mech.*, 123(12), 1219–1229.
- Rubinstein, R. Y. (1981). *Simulation and the Monte-Carlo method*, Wiley, New York.
- Schuëller, G. I., Pradlwarter, H. J., and Pandey, M. D. (1993). "Methods for reliability assessment of nonlinear systems under stochastic dynamic loading—A review." *Proc., EURO-DYN'93*, Balkema, The Netherlands, 751–759.
- Schuëller, G. I., and Stix, R. (1987). "A critical appraisal of methods to determine failure probabilities." *Struct. Safety*, 4, 293–309.
- Structural Engineers Association of California (SEAOC 1995). (2000). "Vision 2000: Performance based seismic engineering of buildings." *Technical Rep.*, Structural Engineers Association of California, Sacramento, Calif.
- Silverman, B. W. (1986). *Density estimators*, Chapman and Hall, New York.
- Wen, Y. K. (2000). "Reliability and performance based design." *Proc., 8th ASCE Specialty Conf. on Probabilistic Mechanics and Structural Reliability*, ASCE, Notre Dame, Ind.